

A μ - τ -philic Higgs doublet confronted with the muon $g-2$, τ decays and LHC data

Lei Wang¹, Yang Zhang²

¹ *Department of Physics, Yantai University, Yantai 264005, P. R. China*

² *ARC Centre of Excellence for Particle Physics at the Tera-scale,
School of Physics and Astronomy, Monash University,
Melbourne, Victoria 3800, Australia*

Abstract

In the framework of the two-Higgs-doublet model, one Higgs doublet may have the same interactions with fermions as the SM, and another Higgs doublet only has the μ - τ LFV interactions. Assuming that the Yukawa matrices are real and symmetrical, we impose various relevant theoretical and experimental constraints, and find that the excesses of muon $g - 2$ and lepton flavour universality in the τ decays can be simultaneously explained in the region of small mass splittings between the heavy CP-even Higgs and the CP-odd Higgs ($m_A > m_H$). The multi-lepton event searches at the LHC can sizably reduce the mass ranges of extra Higgses, and m_H is required to be larger than 560 GeV.

I. INTRODUCTION

The muon anomalous magnetic moment $g - 2$ has been a long-standing puzzle since the announcement by the E821 experiment in 2001 [1]. There is an almost 3.7σ discrepancy between the experimental value and the prediction of the SM [2]

$$\Delta a_\mu = a_\mu^{exp} - a_\mu^{SM} = (274 \pm 73) \times 10^{-11}. \quad (1)$$

The lepton flavor universality (LFU) in the τ decays is an excellent way to probe new physics. The HFAG collaboration reported three ratios from pure leptonic processes, and two ratios from semi-hadronic processes, $\tau \rightarrow \pi/K\nu$ and $\pi/K \rightarrow \mu\nu$ [3]

$$\begin{aligned} \left(\frac{g_\tau}{g_\mu}\right) &= 1.0011 \pm 0.0015, & \left(\frac{g_\tau}{g_e}\right) &= 1.0029 \pm 0.0015, \\ \left(\frac{g_\mu}{g_e}\right) &= 1.0018 \pm 0.0014, & \left(\frac{g_\tau}{g_\mu}\right)_\pi &= 0.9963 \pm 0.0027, \\ \left(\frac{g_\tau}{g_\mu}\right)_K &= 0.9858 \pm 0.0071, \end{aligned} \quad (2)$$

where the ratios of $\left(\frac{g_\tau}{g_e}\right)$ and $\left(\frac{g_\tau}{g_\mu}\right)_K$ have approximate 2σ discrepancy from the SM.

As a simple extension of the SM, the lepton-specific two-Higgs-doublet model (2HDM) can accommodate the muon $g - 2$ anomaly by the contributions of two-loop Barr-Zee diagrams for a light CP-odd Higgs A and large $\tan\beta$ [4–15]. However, the tree-level diagram mediated by the charged Higgs gives negative contribution to the decay $\tau \rightarrow \mu\nu\bar{\nu}$, which will raise the deviation of the LFU in τ decays [10, 12, 16]. In addition, a scalar with the μ - τ LFV interactions can accommodate the muon $g - 2$ anomaly by the contribution of one-loop diagrams [17–23]. Recently, Ref. [23] showed that the excesses of muon $g - 2$ and LFU in τ decays can be simultaneously explained in the 2HDM in which one Higgs doublet has the same interactions with fermions as the SM, and another Higgs doublet only has the μ - τ LFV interactions. In this paper, we focus on applying the ATLAS and CMS direct searches at the LHC to constrain the parameter space explaining the excesses of muon $g - 2$ and LUF in τ decays.

Our work is organized as follows. In Sec. II we recapitulate the model. In Sec. III we discuss the muon $g - 2$, LUF in τ decays, and other relevant constraints, and then use the direct search limits at the LHC to constrain the model. Finally, we give our conclusion in Sec. IV.

TABLE I: The Z_4 charge assignment.

	Q_L^i	U_R^i	D_R^i	L_L^e	L_L^μ	L_L^τ	e_R	μ_R	τ_R	Φ_1	Φ_2
Z_4	1	1	1	1	i	$-i$	1	i	$-i$	1	-1

II. THE 2HDM WITH μ - τ -PHILIC HIGGS DOUBLET

In Ref. [23], an inert Higgs doublet Φ_2 is introduced to the SM under an abelian discrete Z_4 symmetry, and the Z_4 charge assignment is shown in Table I. The scalar potential of Φ_2 and Φ_1 is given as

$$\begin{aligned}
 V = & Y_1(\Phi_1^\dagger \Phi_1) + Y_2(\Phi_2^\dagger \Phi_2) + \frac{\lambda_1}{2}(\Phi_1^\dagger \Phi_1)^2 + \frac{\lambda_2}{2}(\Phi_2^\dagger \Phi_2)^2 \\
 & + \lambda_3(\Phi_1^\dagger \Phi_1)(\Phi_2^\dagger \Phi_2) + \lambda_4(\Phi_1^\dagger \Phi_2)(\Phi_2^\dagger \Phi_1) \\
 & + \left[\frac{\lambda_5}{2}(\Phi_1^\dagger \Phi_2)^2 + \text{h.c.} \right].
 \end{aligned} \tag{3}$$

We focus on the CP-conserving case, and all λ_i are real. The two complex scalar doublets can be written as

$$\Phi_1 = \begin{pmatrix} G^+ \\ \frac{1}{\sqrt{2}}(v + h + iG^0) \end{pmatrix}, \quad \Phi_2 = \begin{pmatrix} H^+ \\ \frac{1}{\sqrt{2}}(H + iA) \end{pmatrix}.$$

The Φ_1 field has the vacuum expectation value (VEV) $v=246$ GeV, and the VEV of Φ_2 field is zero. We determine Y_1 by requiring the scalar potential minimization condition.

$$Y_1 = -\frac{1}{2}\lambda_1 v^2. \tag{4}$$

The G^0 and G^+ are the Nambu-Goldstone bosons which are eaten by the gauge bosons. The H^+ and A are the mass eigenstates of the charged Higgs boson and CP-odd Higgs boson. Their masses are given as

$$m_{H^\pm}^2 = Y_2 + \frac{\lambda_3}{2}v^2, \quad m_A^2 = m_{H^\pm}^2 + \frac{1}{2}(\lambda_4 - \lambda_5)v^2. \tag{5}$$

The two CP-even Higgses h and H are mass eigenstates, and there is no mixing between them. In this paper, the light CP-even Higgs h is taken as the SM-like Higgs. Their masses are given as

$$m_h^2 = \lambda_1 v^2 \equiv (125 \text{ GeV})^2, \quad m_H^2 = m_A^2 + \lambda_5 v^2. \tag{6}$$

The masses of fermions are obtained from the Yukawa interactions with Φ_1 ,

$$-\mathcal{L} = y_u \bar{Q}_L \tilde{\Phi}_1 U_R + y_d \bar{Q}_L \Phi_1 D_R + y_\ell \bar{L}_L \Phi_1 E_R + \text{h.c.}, \tag{7}$$

where $\tilde{\Phi}_1 = i\tau_2\Phi_1^*$, $Q_L^T = (u_{Li}, d_{Li})$, $L_L^T = (\nu_{Li}, \ell_{Li})$ with i being generation indices. U_R , D_R , and E_R denote the three generation right-handed fields of the up-type quark, down-type quark, and charged lepton. According to the Z_4 charge assignment in Table I, the Z_4 symmetry allows the quark Yukawa matrix y_u (y_d) to be not diagonalized, and requires the lepton Yukawa matrix y_ℓ to be diagonal. Therefore, the quark fields (Q_L , U_R , D_R) are the interaction eigenstates, and the lepton fields (L_L , E_R) are mass eigenstates.

The Z_4 symmetry allows Φ_2 to have μ - τ interactions [23],

$$-\mathcal{L}_{LFV} = \sqrt{2} \rho_{\mu\tau} \overline{L}_L^\mu \Phi_2 \tau_R + \sqrt{2} \rho_{\tau\mu} \overline{L}_L^\tau \Phi_2 \mu_R + \text{h.c.} \quad (8)$$

From Eq. (8), we can obtain μ - τ LFV couplings of extra Higgses (H , A , and H^\pm). We assume that the Yukawa matrix of Φ_2 is CP-conserving, namely that $\rho_{\mu\tau}$ and $\rho_{\tau\mu}$ are real and $\rho_{\mu\tau} = \rho_{\tau\mu} \equiv \rho$.

At the tree-level, the light CP-even Higgs h has the same couplings to fermions and gauge boson as the SM, and the μ - τ LFV coupling of h is absent. The Yukawa couplings of H , A , and H^\pm are μ - τ -philic, and they have no other Yukawa couplings. The neutral Higgses A and H have no cubic interactions with ZZ , WW .

III. MUON $g - 2$, LUF IN τ DECAYS, LHC DATA, AND RELEVANT CONSTRAINTS

A. Numerical calculations

In our calculations, we take λ_2 , λ_3 , m_h , m_H , m_A and m_{H^\pm} as the input parameters, which can determine the values of λ_1 , λ_5 and λ_4 from Eqs. (5, 6). λ_2 controls the quartic couplings of extra Higgses, and does not affect the observables considered in our paper. Therefore, we simply take $\lambda_2 = \lambda_1$. λ_3 is adjusted to satisfy the theoretical constraints. We fix $m_h = 125$ GeV, and scan over several key parameters in the following ranges:

$$\begin{aligned} 300 \text{ GeV} < m_H < 800 \text{ GeV}, \quad m_H < m_A = m_{H^\pm} < m_H + 200 \text{ GeV}, \\ 0.1 < \rho < 1.0. \end{aligned} \quad (9)$$

At the tree-level, the SM-like Higgs has the same couplings to the SM particles as the SM, and no exotic decay mode for such Higgs mass spectrum. The masses of extra Higgses

are beyond the exclusion range of the searches for the neutral and charged Higgs at the LEP. Because the extra Higgses have no couplings to quarks, the bounds from meson observables can be safely neglected.

In our calculation, we consider the following observables and constraints:

- (1) Theoretical constraints and precision electroweak data. The 2HDMC [24] is employed to implement the theoretical constraints from the vacuum stability, unitarity and coupling-constant perturbativity, and calculated the oblique parameters (S , T , U). Adopting the recent fit results in Ref. [25], we use the following values of S , T , U ,

$$S = 0.02 \pm 0.10, \quad T = 0.07 \pm 0.12, \quad U = 0.00 \pm 0.09. \quad (10)$$

The correlation coefficients are given by

$$\rho_{ST} = 0.92, \quad \rho_{SU} = -0.66, \quad \rho_{TU} = -0.86. \quad (11)$$

The oblique parameters favor that one of H and A has a small mass splitting from H^\pm , and therefore we simply take $m_A = m_{H^\pm}$ in this paper.

- (2) Muon $g - 2$. The model contributes to the muon $g - 2$ through the one-loop diagrams involving the μ - τ LFV coupling of H and A [18],

$$\delta a_\mu = \frac{m_\mu m_\tau \rho^2}{8\pi^2} \left[\frac{(\log \frac{m_H^2}{m_\tau^2} - \frac{3}{2})}{m_H^2} - \frac{\log(\frac{m_A^2}{m_\tau^2} - \frac{3}{2})}{m_A^2} \right]. \quad (12)$$

From Eq. (12), the model can give a positive contribution to the muon $g - 2$ for $m_A > m_H$. This is reason why we scan over the parameter space of $m_A > m_H$.

- (3) Lepton universality in the τ decays. The HFAG collaboration reported three ratios from pure leptonic processes,

$$\begin{aligned} \left(\frac{g_\tau}{g_\mu} \right)^2 &\equiv \bar{\Gamma}(\tau \rightarrow e\nu\bar{\nu})/\bar{\Gamma}(\mu \rightarrow e\nu\bar{\nu}), \\ \left(\frac{g_\tau}{g_e} \right)^2 &\equiv \bar{\Gamma}(\tau \rightarrow \mu\nu\bar{\nu})/\bar{\Gamma}(\mu \rightarrow e\nu\bar{\nu}), \\ \left(\frac{g_\mu}{g_e} \right)^2 &\equiv \bar{\Gamma}(\tau \rightarrow \mu\nu\bar{\nu})/\bar{\Gamma}(\tau \rightarrow e\nu\bar{\nu}), \end{aligned} \quad (13)$$

and two ratios from semi-hadronic processes, $\tau \rightarrow \pi/K\nu$ and $\pi/K \rightarrow \mu\nu$ [3]. The values of five ratios are given in Eq. (2). Here $\bar{\Gamma}$ denotes the partial width normalized to its SM value. The correlation matrix for the above five observables is

$$\begin{pmatrix} 1 & +0.53 & -0.49 & +0.24 & +0.12 \\ +0.53 & 1 & +0.48 & +0.26 & +0.10 \\ -0.49 & +0.48 & 1 & +0.02 & -0.02 \\ +0.24 & +0.26 & +0.02 & 1 & +0.05 \\ +0.12 & +0.10 & -0.02 & +0.05 & 1 \end{pmatrix}. \quad (14)$$

In this model,

$$\begin{aligned} \bar{\Gamma}(\tau \rightarrow \mu\nu\bar{\nu}) &= (1 + \delta_{\text{loop}}^\tau)^2 (1 + \delta_{\text{loop}}^\mu)^2 + \delta_{\text{tree}}, \\ \bar{\Gamma}(\tau \rightarrow e\nu\bar{\nu}) &= (1 + \delta_{\text{loop}}^\tau)^2, \\ \bar{\Gamma}(\mu \rightarrow e\nu\bar{\nu}) &= (1 + \delta_{\text{loop}}^\mu)^2. \end{aligned} \quad (15)$$

Where δ_{tree} can give a positive correction to $\tau \rightarrow \mu\nu\bar{\nu}$, and is from the tree-level diagram mediated by the charged Higgs,

$$\delta_{\text{tree}} = 4 \frac{m_W^4 \rho^4}{g^4 m_{H^\pm}^4}. \quad (16)$$

$\delta_{\text{loop}}^\tau$ and δ_{loop}^μ denote the corrections to vertices $W\bar{\nu}_\tau\tau$ and $W\bar{\nu}_\mu\mu$, respectively, which are from the one-loop diagrams involving H , A , and H^\pm . Since we take $X_{\mu\tau} = X_{\tau\mu}$ for the lepton Yukawa matrix, and therefore $\delta_{\text{loop}}^\tau = \delta_{\text{loop}}^\mu$. Following results of [10, 12, 23],

$$\delta_{\text{loop}}^\tau = \delta_{\text{loop}}^\mu = \frac{1}{16\pi^2} \rho^2 \left[1 + \frac{1}{4} (H(x_A) + H(x_H)) \right], \quad (17)$$

where $H(x_\phi) \equiv \ln(x_\phi)(1 + x_\phi)/(1 - x_\phi)$ with $x_\phi = m_\phi^2/m_{H^\pm}^2$.

In the model,

$$\left(\frac{g_\tau}{g_\mu} \right)_\pi = \left(\frac{g_\tau}{g_\mu} \right)_K = \left(\frac{g_\tau}{g_\mu} \right). \quad (18)$$

We perform χ_τ^2 calculation for the five observables. The covariance matrix constructed from the data of Eq. (2) and Eq. (14) has a vanishing eigenvalue, and the corresponding degree is removed in our calculation.

- (4) Lepton universality in the Z decays. The measured values of the ratios of the leptonic Z decay branching fractions are given as [26]:

$$\frac{\Gamma_{Z \rightarrow \tau^+ \tau^-}}{\Gamma_{Z \rightarrow e^+ e^-}} = 1.0019 \pm 0.0032, \quad (19)$$

$$\frac{\Gamma_{Z \rightarrow \mu^+ \mu^-}}{\Gamma_{Z \rightarrow e^+ e^-}} = 1.0009 \pm 0.0028, \quad (20)$$

with a correlation of +0.63. The model can give corrections to the widths of $Z \rightarrow \tau^+ \tau^-$ and $Z \rightarrow \mu^+ \mu^-$ through the one-loop diagrams involving the extra Higgs bosons. The quantities of Eq. (19) are calculated in the model as [10, 12, 23]

$$\frac{\Gamma_{Z \rightarrow \tau^+ \tau^-}}{\Gamma_{Z \rightarrow e^+ e^-}} \approx 1.0 + \frac{2g_L^e \text{Re}(\delta g_L^{\text{loop}}) + 2g_R^e \text{Re}(\delta g_R^{\text{loop}})}{g_L^e{}^2 + g_R^e{}^2}. \quad (21)$$

where the SM value $g_L^e = -0.27$ and $g_R^e = 0.23$. δg_L^{loop} and δg_R^{loop} are from the one-loop corrections, which are given as

$$\delta g_L^{\text{loop}} = \frac{1}{16\pi^2} \rho^2 \left\{ -\frac{1}{2} B_Z(r_A) - \frac{1}{2} B_Z(r_H) - 2C_Z(r_A, r_H) + s_W^2 \left[B_Z(r_A) + B_Z(r_H) + \tilde{C}_Z(r_A) + \tilde{C}_Z(r_H) \right] \right\}, \quad (22)$$

$$\delta g_R^{\text{loop}} = \frac{1}{16\pi^2} \rho^2 \left\{ 2C_Z(r_A, r_H) - 2C_Z(r_{H^\pm}, r_{H^\pm}) + \tilde{C}_Z(r_{H^\pm}) - \frac{1}{2} \tilde{C}_Z(r_A) - \frac{1}{2} \tilde{C}_Z(r_H) + s_W^2 [B_Z(r_A) + B_Z(r_H) + 2B_Z(r_{H^\pm}) + \tilde{C}_Z(r_A) + \tilde{C}_Z(r_H) + 4C_Z(r_{H^\pm}, r_{H^\pm})] \right\}, \quad (23)$$

where $r_\phi = m_\phi^2/m_Z^2$ with $\phi = A, H, H^\pm$, and

$$B_Z(r) = -\frac{\Delta_\epsilon}{2} - \frac{1}{4} + \frac{1}{2} \log(r), \quad (24)$$

$$C_Z(r_1, r_2) = \frac{\Delta_\epsilon}{4} - \frac{1}{2} \int_0^1 dx \int_0^x dy \log[r_2(1-x) + (r_1-1)y + xy], \quad (25)$$

$$\tilde{C}_Z(r) = \frac{\Delta_\epsilon}{2} + \frac{1}{2} - r[1 + \log(r)] + r^2[\log(r) \log(1+r^{-1}) - \text{Li}_2(-r^{-1})] - \frac{i\pi}{2} [1 - 2r + 2r^2 \log(1+r^{-1})]. \quad (26)$$

Due to $X_{\mu\tau} = X_{\tau\mu}$, we can obtain

$$\frac{\Gamma_{Z \rightarrow \mu^+ \mu^-}}{\Gamma_{Z \rightarrow e^+ e^-}} = \frac{\Gamma_{Z \rightarrow \tau^+ \tau^-}}{\Gamma_{Z \rightarrow e^+ e^-}}. \quad (27)$$

(5) The exclusions from the ATLAS and CMS searches at the LHC. The extra Higgs bosons are dominantly produced at the LHC via the following electroweak processes:

$$pp \rightarrow W^{\pm*} \rightarrow H^{\pm} A, \quad (28)$$

$$pp \rightarrow Z^* \rightarrow H A, \quad (29)$$

$$pp \rightarrow W^{\pm*} \rightarrow H^{\pm} H, \quad (30)$$

$$pp \rightarrow Z^*/\gamma^* \rightarrow H^+ H^-. \quad (31)$$

For small mass splitting among H , A , and H^{\pm} , the dominant decay modes of these Higgses are

$$H \rightarrow \tau^{\pm} \mu^{\mp}, \quad A \rightarrow \tau^{\pm} \mu^{\mp}, \quad H^{\pm} \rightarrow \tau^{\pm} \nu_{\mu}, \mu^{\pm} \nu_{\tau}. \quad (32)$$

When m_A and $m_{H^{\pm}}$ are much larger than m_H , the following exotic decay modes will open with $m_A = m_{H^{\pm}}$,

$$A \rightarrow H Z, \quad H^{\pm} \rightarrow H W^{\pm}. \quad (33)$$

In order to restrict the productions of the above processes at the LHC for our model, we perform simulations for the samples using `MG5_aMC-2.4.3` [27] with `PYTHIA6` [28] and `Delphes-3.2.0` [29], and adopt the constraints from all the analysis for the 13 TeV LHC in version `CheckMATE 2.0.26` [30]. Besides, the latest multi-lepton searches for electroweakino [31–35] implemented in Ref. [36] and the ATLAS search for direct stau production with 139 fb⁻¹ 13 TeV events [37] are also taken into consideration.

B. Results and discussions

We find that the constraints from theory, oblique parameters and Z decays can be easily satisfied in the parameter space taken in this paper. The allowed ranges of m_H , m_A , $m_{H^{\pm}}$, and ρ are not reduced by the those constraints. Therefore, we won't show their results in the following discussions.

After imposing the constraints of the theory, the oblique parameters, and Z decays, in Fig. 1 we show the surviving samples which are consistent with Δa_{μ} and τ decays at 2σ level. The contributions of H and A to Δa_{μ} are respectively positive and negative, and a large mass splitting between m_A and m_H can produce sizable corrections to Δa_{μ} . Thus, with

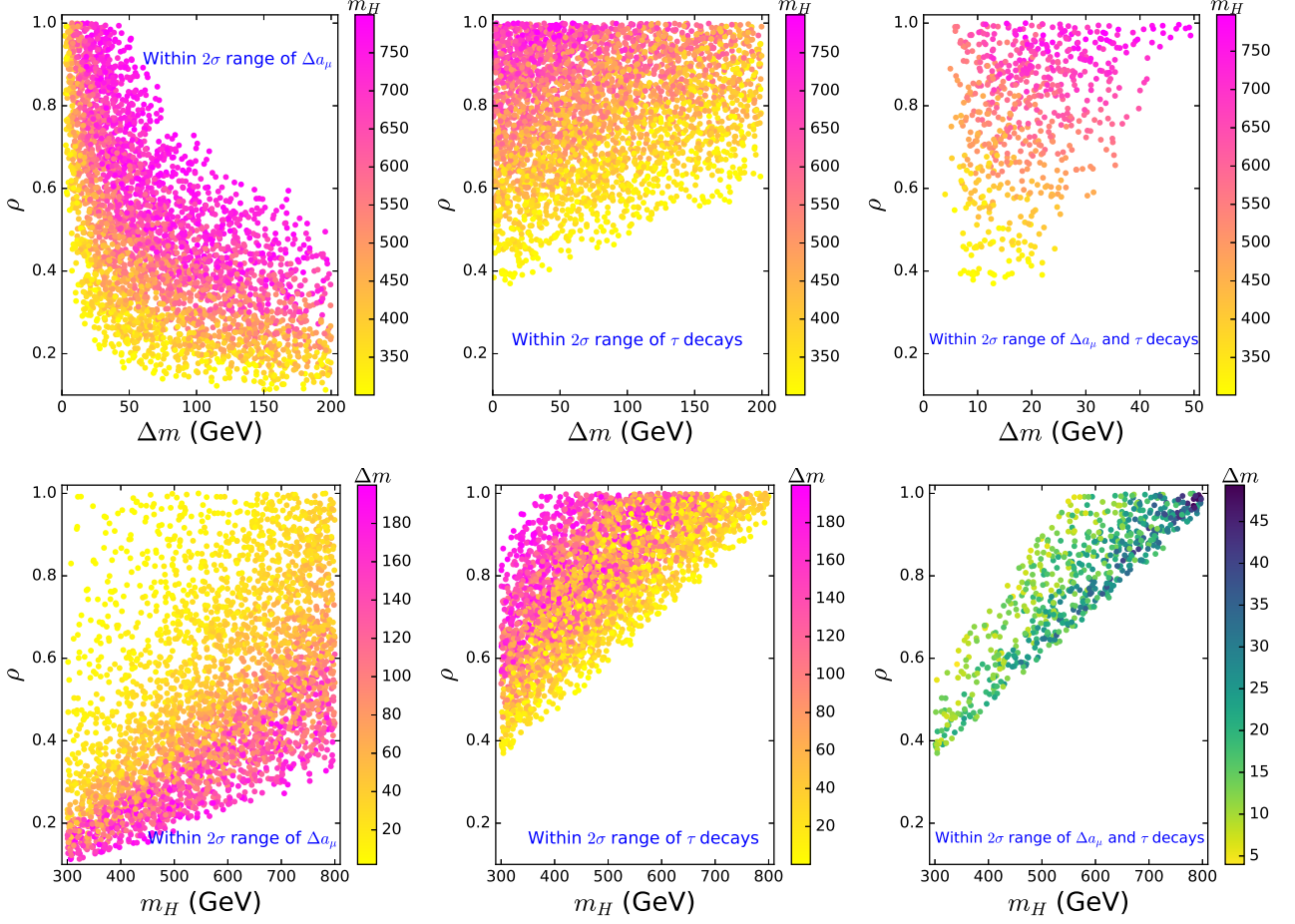


FIG. 1: The samples within 2σ ranges of Δa_μ (left panel), LUF in the τ decays (middle panel), and both Δa_μ and LUF in the τ decays (right panel). All the samples satisfy the constraints of the theory, oblique parameters and Z decays. Here $\Delta m \equiv m_A(m_{H^\pm}) - m_H$.

an increase of Δm , a relative small ρ can make Δa_μ to be within 2σ range of experimental data, as shown in upper-left panel in Fig. 1.

The experimental value of $\left(\frac{g_\tau}{g_e}\right)$ has about 2σ positive deviation from the SM prediction. Enhancement of $\Gamma(\tau \rightarrow \mu\nu\bar{\nu})$ can provide a better fit. According to Eq. (15), the δ_{tree} term can enhance $\Gamma(\tau \rightarrow \mu\nu\bar{\nu})$, and favor ρ to increase with m_{H^\pm} , see Eq. (16). Therefore, the upper-middle panel shows that the experimental data of LFU in the τ decays favor ρ to increase with Δm . Because of the opposite relationship between ρ and Δm , the excesses of Δa_μ and τ decays can be simultaneously explained in a narrow region of ρ and Δm . As shown in the upper-right panel, $\Delta m < 50$ GeV and $\rho > 0.36$ are required, and ρ is favored to increase with Δm .

The lower panels of Fig. 1 show that the experimental data of Δa_μ and τ decays favor ρ to increase with m_H . The lower-right panel shows that the excesses of Δa_μ and τ decays can be simultaneously explained in the range of $300 \text{ GeV} < m_H < 800 \text{ GeV}$, and the corresponding ρ is imposed upper and lower bounds. Taking $m_H = 500 \text{ GeV}$ for an example, the excesses of Δa_μ and LUF in the τ decays can be simultaneously explained for $0.6 < \rho < 0.9$. For $m_H = 500 \text{ GeV}$ and $\rho < 0.6$, Δa_μ can be explained, but the τ decays can not be accommodated. For $m_H = 500 \text{ GeV}$ and $\rho > 0.9$, Δa_μ and the τ decays can be respectively explained. However, the former favors a small Δm and the latter favors a large Δm , which leads that the two anomalies can not be simultaneously explained for $m_H = 500 \text{ GeV}$ and $\rho > 0.9$.

After imposing the constraints of the direct searches at the LHC, those samples of Fig. 1 are projected on the planes of m_H versus ρ and m_H versus Δm , as shown in Fig. 2. Since the excesses of Δa_μ and τ decays require the mass splitting between m_A (m_{H^\pm}) and m_H to be smaller than 50 GeV , H , A and H^\pm will dominantly decay into $\tau\mu$, $\tau\nu_\mu$, and $\mu\nu_\tau$. The direct searches at the LHC exclude region of $m_H < 560 \text{ GeV}$, and the corresponding ρ is required to be larger than 0.68 . Since Δm is such small, it hardly affects the excluded region.

For the excluded samples, the most sensitive experimental analysis is the CMS search for electroweak production of charginos and neutralinos in multilepton final states [33] at 13 TeV LHC with 35.9 fb^{-1} integrated luminosity data. In this analysis, hundreds of signal region bins are designed, of which the **SR-A44** and **SR-C18** provide strongest constraints on our samples. In the **SR-A44**, events are selected on the condition that contains three leptons forming at least one opposite-sign same-flavor (OSSF) pair, $M_{\ell\ell} > 105 \text{ GeV}$, $p_T^{\text{miss}} > 200 \text{ GeV}$ and $M_T > 160 \text{ GeV}$. Here $M_{\ell\ell}$ is the invariant mass of the OSSF dilepton pair, p_T^{miss} stands the missing transverse momentum, and $M_T = \sqrt{2p_T^{\text{miss}}p_T^\ell[1 - \cos(\Delta\phi)]}$ is the transverse mass computed with respect to the third lepton in the event. The **SR-C** is built from events with two e or μ forming an OSSF pair and a hadronic decay tau lepton τ_h . The bin **SR-C18** requires $p_T^{\text{miss}} > 200 \text{ GeV}$, $|M_{\ell\ell} - m_Z| > 15 \text{ GeV}$ and $M_{T2} > 100 \text{ GeV}$. The two-lepton transverse mass M_{T2} [38, 39] is computed with the OSSF pair of light leptons. The main contributions of our samples to the bins are from processes in Eq. (28) and Eq. (30) with one or two of the τ s decaying hadronically. Thus, the exclusion power decreases gently with heavier m_H and M_A due to the smaller production rates for the processes, as shown in the

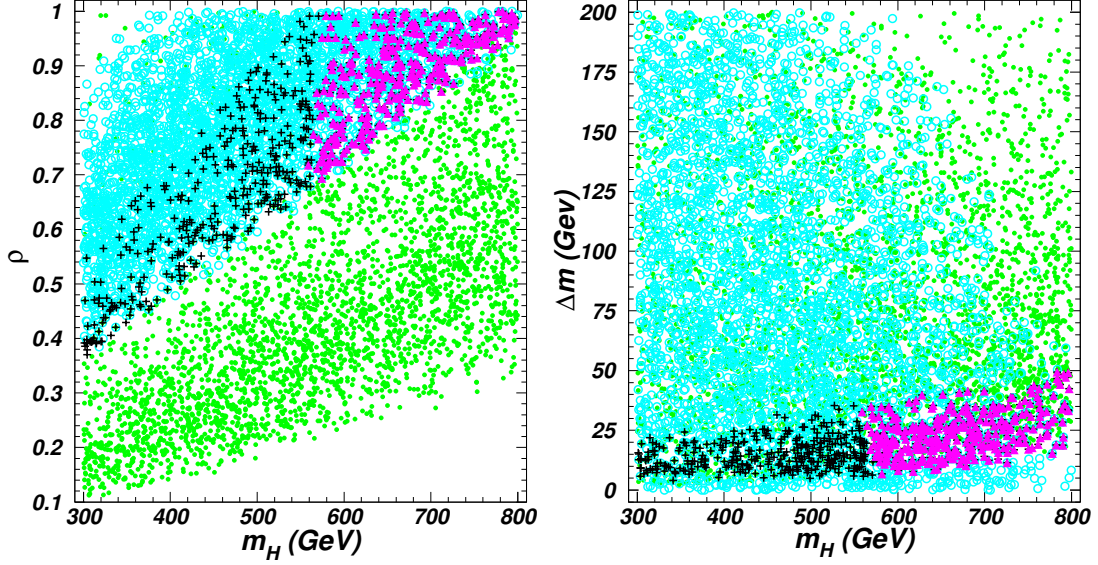


FIG. 2: The surviving samples on the planes of m_H versus ρ and m_H versus Δm . All the samples satisfy the constraints of the theory, oblique parameters and Z decays. In addition, the bullets (green) within the 2σ ranges of muon $g-2$ and the circles (blue) within the 2σ ranges of LUF in the τ decays. The pluses (black) and triangles (purple) are within the 2σ ranges of both muon $g-2$ and LUF in the τ decays, and the former are excluded by the constraints of the direct searches at the LHC, while the latter are allowed.

left panel of Fig. 3, where the y -axis R stands the ratio of event yields in the signal region to the corresponding 95% experimental limit.

We also adopt the ATLAS searches with 139 fb^{-1} integrated luminosity data for slepton pair production [46] and direct stau pair production [37] by implementing them in **CheckMATE** 2.0.26. Although the integrated luminosity is much higher than that of the multilepton search [33], the exclusion powers of the slepton search, which requires exactly two light leptons in final state, and the stau search are weaker than the above constraints. We can see from the left panel of Fig. 3 that the most sensitive signal region in the slepton search is the SR-SF-1J ($m_{T2} > 160 \text{ GeV}$), which can exclude samples of $m_H < 501 \text{ GeV}$. In the SR-SF-1J ($m_{T2} > 160 \text{ GeV}$), events are required to have exactly two light flavour leptons and exactly one jet. Thus the dominated processes for this signal region are Eq. (28) and Eq. (30), where the H^\pm provides one μ and A or H contributes one μ and one τ jet. Note that this bound, $m_H > 501 \text{ GeV}$, is weaker than the estimated limit, $m_\phi > 700 \text{ GeV}$, adopted in Ref. [23], which is the slepton mass bound in the massless neutralino limit [46].

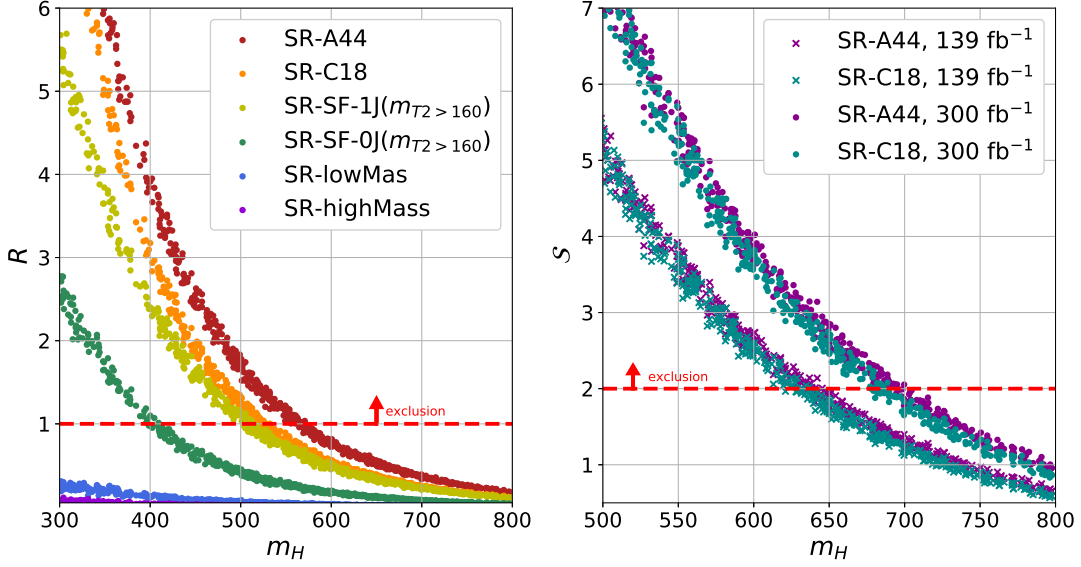


FIG. 3: Left panel: the ratio R of event yields in the signal regions to the corresponding 95% experimental limit for the surviving samples. The red and orange dots represent the signal regions SR-A44 and SR-C18 of the multilepton search with 35.9 fb^{-1} LHC data [33]. The yellow and green dots stand the signal regions SR-SF-1J ($m_{T2} > 160 \text{ GeV}$) and SR-SF-0J ($m_{T2} > 160 \text{ GeV}$) of the sleptons search of two leptons with 139 fb^{-1} LHC data [46]. The green and blue dots represent the signal regions SR-lowMass and SR-highMass of the stau search with 139 fb^{-1} LHC data [37]. Right panel: the estimated expected significance \mathcal{S} for the surviving sample with high integrated luminosity. The purple and cyan dots stand the signal regions SR-A44 and SR-C18 with 139 fb^{-1} integrated luminosity data (crosses) and 300 fb^{-1} integrated luminosity data (dots).

The detailed explanations are given in the Appendix.

As for the stau search [37], it can not give constraints to any sample with $m_H > 300 \text{ GeV}$. It is because that both the signal regions, SR-lowMass and SR-highMass, require exactly two taus with opposite-sign electric charge, and reject events with an additional third τ or light lepton. So only process in Eq. (31) could contribute to the signal regions. The other searches corresponding to an integrated luminosity of 139 fb^{-1} face the similar issues, such as requiring multiple jets [40–42], hard jet [43, 44], b-tagged jet [45], or exactly two light flavor leptons [43].

Given the fact that hundred of integrated luminosity 13 TeV events have been recorded at

LHC, we further estimate the exclusion power of LHC with higher luminosity by normalizing signal and background event yields in the signal regions SR-A44 and SR-C18 of [33]. We compute the significance as $\mathbf{S} = \sqrt{2(n_s + n_b) \ln(1 + n_s/n_b) - 2n_s}$, where n_s and n_b are the normalized signal and background event yields, respectively. We show the result in the right panel of Fig. 3. The samples with $m_H < 645$ (700) GeV will be excluded at 2σ confidence level with 139 (300) fb^{-1} integrated luminosity data. If the signal regions of [33] are optimized for the production and decay modes in Eq. (28-32), the detection ability of LHC for this model could be further enhanced.

IV. CONCLUSION

In this paper, we discuss a 2HDM in which one Higgs doublet has the same interactions with fermions as the SM, and another Higgs doublet only has the $\mu\text{-}\tau$ LFV interactions. Assuming the Yukawa matrices to be real and symmetrical, we considered various relevant theoretical and experimental constraints, and found that the excesses of muon $g - 2$ and LUF in the τ decays can be simultaneously explained in many parameter spaces with $300 \text{ GeV} < m_H < 800 \text{ GeV}$, $\Delta m < 50 \text{ GeV}$, and $0.36 < \rho < 1$. The parameter spaces are sizable reduced by the direct search limits from the LHC, and m_H is required to be larger than 560 GeV.

Note added: When this manuscript is being prepared, a similar paper appeared in the arXiv [47]. Here we discussed different scenario, and obtain different conclusions.

Acknowledgment

This work was supported by the Natural Science Foundation of Shandong province (ZR2017JL002 and ZR2017MA004), by the National Natural Science Foundation of China under grant 11575152, 11975013, and by the ARC Centre of Excellence for Particle Physics at the Tera-scale under the grant CE110001004.

Appendix

In this appendix, we explain in detail why the constraints from the ATLAS searches for two leptons and E_T^{miss} [46] on Higgs masses in our model are weaker than that on slepton masses in the simplified model where only mass-degenerate \tilde{e} and $\tilde{\mu}$ are considered. In Table II, we compare the cross sections, cut flows and event yield in each signal regions for a benchmark point in the simplified model, $(m_{\tilde{e}}, m_{\tilde{\chi}_1^0}) = (700, 0)$ GeV, and a point in our model, $m_H = m_A = m_{H^\pm} = 700$ GeV.

We can see that the dominated process for our model are the Eq. (28) and Eq. (30), i.e. $pp \rightarrow H^\pm A$, $H^\pm H$, and the cross section is larger than that of slepton pair production when $m_{H/A/H^\pm} = m_{\tilde{e}}$. However, for slepton pair production, the cut efficiency ϵ of each step is quit large, which means only small part of events are discarded. Furthermore, the surviving events are all assigned into same-flavour (SF) signal regions. While, for the Higgs production, requiring 2 opposite-sign (OS) leptons and number of jets n_{jets} less than 2 rejects most of the events, and the rest of events are separated into both SF and different-flavour (DF) signal regions. It is because that the final states of $H^\pm H(A)$ are either $1\mu + 2\tau$ or $2\mu + 1\tau$. For $1\mu + 2\tau$ final state, when both of the τ s decay hadronically or leptonically, the events will be rejected. The event with $2\mu + 1\tau$ final state where τ decaying leptonically also can not pass the 2 lepton requirement. Meanwhile, there is a possibility that the remaining two lepton are same-sign. Furthermore, the hadronic τ leads to an additional jet, which will decrease the possibility that the event passes the requirement of $n_{\text{jets}} < 2$ because there may be initial state radiation jet. The lepton from leptonic decay of τ can be e or μ , which means that the event will be allocated into SF or DF signal regions. As a result, the normalised events number N in the most sensitive signal region, **SR-SF-1J** ($m_{T2} > 160$ GeV), of slepton pair production is much larger than that of Higgs production in our model.

-
- [1] H. N. Brown et al. [Muon g-2 Collaboration], Phys. Rev. Lett. **86**, (2001) 2227.
 - [2] T. Blum et al. [RBC and UKQCD Collaborations], Phys. Rev. Lett. **121**, (2018) 022003.
 - [3] Y. Amhis et al. [Heavy Flavor Averaging Group (HFAG) Collaboration], arXiv:1412.7515.
 - [4] D. Chang, W.-F. Chang, C.-H. Chou, and W.-Y. Keung, Phys. Rev. D **63**, (2001) 091301.
 - [5] K. M. Cheung, C. H. Chou and O. C. W. Kong, Phys. Rev. D **64**, (2001) 111301.

TABLE II: Cross sections, cut flows and event yields in each signal region for a benchmark point of $(m_{\tilde{\ell}}, m_{\tilde{\chi}_1^0}) = (700, 0)$ GeV in the simplified slepton model and a point in our model with $m_H = m_A = m_{H^\pm} = 700$ GeV. $\tilde{\ell}$ stands the first two generations of mass-degenerate sleptons. “Combine” includes all non-SM Higgs productions in our model. ϵ indicates the cut efficiency and the normalised events number N is the product of cross section, integrated luminosity and ϵ . The signal region name is abbreviated, such as “DF-0J-100” standing SR-DF-0J ($m_{T2} > 100$ GeV).

Process	$\tilde{\ell}^\pm \tilde{\ell}^\mp$		Combine		$H^\pm A, H^\pm H$		$H^\pm H^\mp$		HA	
Cross section (fb)	0.178		0.336		0.218		0.064		0.054	
Cut Flow										
	ϵ	N	ϵ	N	ϵ	N	ϵ	N	ϵ	N
No cut	100%	24.8	100%	46.7	100%	30.3	100%	8.9	100%	7.5
2 OS leptons	90.77%	22.5	31.67%	14.8	31.66%	9.6	38.00%	3.4	25.86%	1.9
$m_{\ell_1 \ell_2} > 100$ GeV	89.54%	22.2	31.13%	14.5	31.21%	9.5	36.84%	3.3	25.48%	1.9
No b-tagged jet	83.75%	20.7	28.34%	13.2	28.37%	8.6	34.54%	3.1	22.54%	1.7
$E_T^{\text{miss}} > 110$ GeV	79.14%	19.6	26.06%	12.2	26.77%	8.1	32.34%	2.9	17.47%	1.3
E_T^{miss} significance > 10	79.14%	19.6	26.06%	12.2	26.77%	8.1	32.34%	2.9	17.47%	1.3
$n_{\text{jets}} < 2$	63.46%	15.7	14.47%	6.8	14.10%	4.3	26.12%	2.3	3.22%	0.2
$m_{\ell_1 \ell_2} > 121.2$ GeV ^a	62.96%	15.6	14.38%	6.7	14.04%	4.3	25.87%	2.3	3.21%	0.2
Signal Regions										
DF-0J-100	0%	0	0.76%	0.4	0.49%	0.1	2.27%	0.2	0.05%	0.0
DF-0J-100-120	0%	0	0.04%	0.0	0.03%	0.0	0.20%	0.0	0.01%	0.0
DF-0J-120-160	0%	0	0.13%	0.1	0.08%	0.0	0.40%	0.0	0.01%	0.0
DF-0J-160	0%	0	0.58%	0.3	0.38%	0.1	1.67%	0.1	0.03%	0.0
DF-1J-100	0%	0	1.67%	0.8	2.08%	0.6	1.52%	0.1	0.31%	0.0
DF-1J-100-120	0%	0	0.14%	0.1	0.16%	0.0	0.13%	0.0	0.02%	0.0
DF-1J-120-160	0%	0	0.26%	0.1	0.32%	0.1	0.29%	0.0	0.06%	0.0
DF-1J-160	0%	0	1.27%	0.6	1.60%	0.5	1.10%	0.1	0.23%	0.0
SF-0J-100	32.89%	8.1	2.68%	1.3	1.24%	0.4	10.43%	0.9	0.17%	0.0
SF-0J-100-120	1.07%	0.3	0.13%	0.1	0.06%	0.0	0.45%	0.0	0.03%	0.0
SF-0J-120-160	2.39%	0.6	0.26%	0.1	0.15%	0.0	0.93%	0.1	0.03%	0.0
SF-0J-160	29.43%	7.3	2.29%	1.1	1.04%	0.3	9.05%	0.8	0.12%	0.0
SF-1J-100	23.48%	5.8	5.95%	2.8	6.60%	2.0	7.05%	0.6	1.72%	0.1
SF-1J-100-120	0.72%	0.2	0.24%	0.1	0.34%	0.1	0.29%	0.0	0.11%	0.0
SF-1J-120-160	1.64%	0.4	0.57%	0.3	0.69%	0.2	0.71%	0.1	0.25%	0.0
SF-1J-160	21.13%	5.2	5.13%	2.4	5.58%	1.7	6.06%	0.5	1.36%	0.1

^aThis cut is only applied to the events with two same-flavour leptons.

[6] K. Cheung and O. C. W. Kong, Phys. Rev. D **68**, (2003) 053003.

[7] J. Cao, P. Wan, L. Wu and J. M. Yang, Phys. Rev. D **80**, (2009) 071701.

[8] A. Broggio, E. J. Chun, M. Passera, K. M. Patel and S. K. Vempati, JHEP **1411**, (2014)

058.

- [9] L. Wang and X. F. Han, JHEP **05**, (2015) 039.
- [10] T. Abe, R. Sato and K. Yagyu, JHEP **1507**, (2015) 064.
- [11] E. J. Chun, Z. Kang, M. Takeuchi, Y.-L. Tsai, JHEP **1511**, (2015) 099.
- [12] E. J. Chun, J. Kim, JHEP **1607**, (2016) 110.
- [13] A. Crivellin, J. Heeck, P. Stoffer, Phys. Rev. Lett. **116**, (2016) 081801.
- [14] L. Wang, J. M. Yang, M. Zheng, Y. Zhang, Phys. Lett. B **788**, (2019) 519-529.
- [15] M. Lindner, M. Platscher, F. S. Queiroz, arXiv:1610.06587.
- [16] X.-F. Han, T. Li, L. Wang, Y. Zhang, Phys. Rev. D **99**, (2019) 095034.
- [17] K. Adikle Assamagan, A. Deandrea, P.-A. Delsart, Phys. Rev. D **67**, (2003) 035001.
- [18] S. Davidson, G. J. Grenier, Phys. Rev. D **81**, (2010) 095016.
- [19] Y. Omura, E. Senaha, K. Tobe, JHEP **1505**, (2015) 028.
- [20] R. Benbrik, C.-H. Chen, T. Nomura, Phys. Rev. D **93**, (2016) 095004.
- [21] Y. Omura, E. Senaha, K. Tobe, Phys. Rev. D **94**, (2016) 055019.
- [22] L. Wang, S. Yang, X.-F. Han, Nucl. Phys. B **919**, (2017) 123-141.
- [23] Y. Abe, T. Toma, K. Tsumura, JHEP **1906**, (2019) 142.
- [24] D. Eriksson, J. Rathsmann, O. Stål, Comput. Phys. Commun. **181**, (2010) 189.
- [25] M. Tanabashi et al., [Particle Data Group], Phys. Rev. D **98**, 030001 (2018).
- [26] S. Schael et al. [ALEPH and DELPHI and L3 and OPAL and SLD and LEP Electroweak Working Group and SLD Electroweak Group and SLD Heavy Flavour Group Collaborations], Phys. Rept. **427**, (2006) 257.
- [27] J. Alwall *et al.*, JHEP **1407**, (2014) 079.
- [28] P. Torrielli and S. Frixione, JHEP **1004**, (2010) 110.
- [29] J. de Favereau *et al.* [DELPHES 3 Collaboration], JHEP **1402**, (2014) 057.
- [30] D. Dercks, N. Desai, J. S. Kim, K. Rolbiecki, J. Tattersall and T. Weber, Comput. Phys. Commun. **221**, (2017) 383.
- [31] A. M. Sirunyan *et al.* [CMS Collaboration], JHEP **1711**, (2017) 029.
- [32] A. M. Sirunyan *et al.* [CMS Collaboration], JHEP **1803**, (2018) 076.
- [33] A. M. Sirunyan *et al.* [CMS Collaboration], JHEP **1803**, (2018) 166.
- [34] A. M. Sirunyan *et al.* [CMS Collaboration], JHEP **1803**, (2018) 160.
- [35] M. Aaboud *et al.* [ATLAS Collaboration], Eur. Phys. J. C **78**, (2018) 154.

- [36] G. Pozzo and Y. Zhang, Phys. Lett. B **789**, (2019) 582-591.
- [37] The ATLAS collaboration [ATLAS Collaboration], ATLAS-CONF-2019-018.
- [38] C. G. Lester and D. J. Summers, Phys. Lett. B **463**, 99 (1999).
- [39] A. Barr, C. Lester and P. Stephens, J. Phys. G **29**, 2343 (2003).
- [40] CMS Collaboration [CMS Collaboration], CMS-PAS-SUS-19-008.
- [41] CMS Collaboration [CMS Collaboration], CMS-PAS-SUS-19-003.
- [42] The ATLAS collaboration [ATLAS Collaboration], ATLAS-CONF-2019-015.
- [43] The ATLAS collaboration [ATLAS Collaboration], ATLAS-CONF-2019-014.
- [44] The ATLAS collaboration [ATLAS Collaboration], ATLAS-CONF-2019-020.
- [45] The ATLAS collaboration [ATLAS Collaboration], ATLAS-CONF-2019-031.
- [46] The ATLAS collaboration [ATLAS Collaboration], ATLAS-CONF-2019-008.
- [47] S. Iguro, Y. Omura, M. Takeuchi, arXiv:1907.09845.